NaK alloy as a versatile reagent for template-free synthesis of porous metal- and metalloid-based nanostructures

Article *in* Chemical Communications · April 2024

DOI: 10.1039/D4CC00966E

CITATIONS
0

READS
80

5 authors, including:

Sergei Leonchuk
ITMO University
5 PUBLICATIONS **16** CITATIONS
SEE PROFILE

Aleksandra Falchevskaya
ITMO University
11 PUBLICATIONS **115** CITATIONS
SEE PROFILE

Polina A. Morozova
Skolkovo Institute of Science and Technology
13 PUBLICATIONS **176** CITATIONS
SEE PROFILE

Nikolai Gromov
ITMO University
1 PUBLICATION **0** CITATIONS
SEE PROFILE

COMMUNICATION

NaK alloy as a versatile reagent for template-free synthesis of porous metal- and metalloid-based nanostructures

Received 28 February 2024,
Accepted 02 April 2024

DOI: 10.1039/D4CC00966E

Sergei S. Leonchuk,[a] Aleksandra S. Falchevskaya,[a] Polina A. Morozova,[b] Nikolai V. Gromov [a] and Vladimir V. Vinogradov [a]*

Using the strong reduction potential of the liquid NaK-78 alloy, we present a new versatile template-free approach to the synthesis of porous metal- and metalloid-based nanomaterials. With this novel approach, NaK can be simultaneously used as an agent for reduction, structure directing, and pore formation without the use of additional reagents.

Functional materials with controllable porous structures are considered promising candidates for various applications in materials science, including heterogeneous catalysis, energy storage, purification, and green chemistry.[1] To support these applications, several simple, versatile, and sustainable solution methods have been developed, including solvothermal and sol-gel synthesis, selective leaching, self-assembly, as well as template and self-template methods.[1–3] However, most of these conventional approaches are very specific and cannot be scaled for analogous systems. In contrast, alternative liquid metal-mediated approaches can be a useful tool for material production.[4,5] For example, Ga and GaIn alloy can be used as agents for metal- and oxide-based porous structures fabrication,[6,7] as well as sacrificial templates and structure-directing agents for the synthesis of hollow-structured materials with various compositions and morphologies.[8–11] Unfortunately, this method remains unsuitable for the production of most metalloids and semiconductors, because the reduction potential of Ga is not high enough. Recent research has shown that NaK alloy, another liquid metal, can be used to address this issue since Na and K have two of the highest reduction potentials among metals (− 2.71 and − 2.931 V, respectively)[12,13] and, thus far, this liquid-metal alloy has been used to obtain mesoporous C, Si, and Ge.[14-17] However, this synthetic approach is still limited, with minimal control over the structure, morphology, and porosity of the resulting materials.

Here, we propose a potential solution to the aforementioned problems by using liquid NaK-78 alloy for simultaneous reduction, structure directing, and pore formation. To do so, we have developed a new, versatile, template-free approach to the synthesis of metal- and metalloid-based porous nanomaterials. A diverse range of functional materials, including C, Si, Ge, Sn, Sb, Fe, Ru, Ta, Nb, Ti, and their oxides, with organised pore structures and specific surface areas ranging from 10 to 2000 m^2 were obtained using the proposed method.

The production of porous materials in our approach is provided by NaK alloy emulsions as sacrificial templates. Thus, the first step of the research was to emulsify the eutectic liquid NaK-78 alloy. Unlike GaIn, the strong reactivity of NaK-78 does not allow it to be emulsified in water, dimethylsulfoxide, or dimethylformamide.[8,9] To overcome this limitation, we selected three organic solvents that are inert to alkali metals and have different densities, viscosities, polarities, and molecular structures as dispersion media (Table S1): n-hexane (an aliphatic hydrocarbon), m-xylene (an aromatic hydrocarbon), and 1,2-dimethoxyethane (DME, an ether). NaK is easily emulsified in these media via sonication under an argon atmosphere in the concentrations of 1 – 50 $mg \cdot mL^{-1}$. All the considered systems can be used for NaK emulsification (droplet size of 0.5 – 100 μm, sedimentation time of 7 – 12 min), and the stability of the emulsions is determined by the solvent used. The most stable emulsions were obtained in xylene at a maximum NaK-78 concentration of 10 $mg \cdot mL^{-1}$. The resulting emulsions were used as reagents for the interfacial chemical reduction of metal and metalloid chlorides in solution according to the following general scheme:

$$n\ M_{(liquid)} + XCl_{n(dissolved)} \rightarrow X_{(solid)}\downarrow + n\ MCl_{(solid)}\downarrow$$

where M is Na or K from the NaK-78 alloy, X is the reducing element (metal or metalloid), and n is the valency of X.

The precursors used in this study are covalent chlorides of metals and metalloids. These compounds are perfect candidates for the proposed approach since they are more

[a] *ITMO University, "Solution Chemistry of Advanced Materials and Technologies" (SCAMT) International Institute, Saint Petersburg 191002, Russian Federation. E-mail: vinogradov@scamt-itmo.ru.*
[b] *Center for Energy Science and Technology, Skolkovo Institute of Science and Technology, Moscow, Russian Federation.*

† Electronic Supplementary Information (ESI) available. See DOI: 10.1039/D4CC00966E

stable than bromides and iodides and more reactive and safer than fluorides and alkoxides.[18,19] The precursors form NaCl and KCl as by-products, which are non-toxic, easy to remove, and potentially could act as pore-forming phases.[14,20] The simplicity of alkaline chloride and organic solvent separation underscore the potential environmental friendliness of the proposed method despites NaK consumption. The use of liquid NaK-78 instead of molten Na or K (which have almost the same chemical properties) is a more sustainable way since it does not require additional energy consumption for heating and thermostating of the reaction media.

In the next step, it was necessary to consider the potential scope of our method. Since NaK is a powerful reducing agent, it is thermodynamically possible to reduce almost any metal and most metalloids if their chlorides are soluble in a viable organic solvent (Figure 1A). This makes the approach a versatile synthetic tool with a wide range of potential products. To demonstrate this, several suitable precursors were selected for the synthesis of C-, Si-, Ge-, Sn-, and Sb-based porous materials, which can be used as energy storage devices, but are difficult to obtain using conventional solution methods.[12] The precursors were dissolved in the solvents to form solutions with concentrations of 10, 25, and 50 mmol·L^{-1} (Table S2). The NaK emulsions, which were used as reducing agents, were then mixed with the precursor solutions (Figure 1B). The NaK-78 alloy was used in excess of 20 mol.% to the precursors to create and maintain the reducing media throughout the synthesis, which was conducted for 20 h. A grey to black (or deep-blue for silicon) colour change indicated the end of the reaction. The residual unreacted NaK-78 was then etched to except the effect of impurities dissolved in the alloy on samples quality. The products were washed and dried (see protocol details in ESI).

Further steps of the research were related with the characterization of resulting materials. The morphologies and elemental compositions of the unprocessed products were investigated using SEM and EDX (Figure 2). Spherical microparticles with hollow and cracked expanded structures were obtained in addition to shapeless nanosized powder (Figure S1). The difference in the structure of microspheres is due to the nature of both the solvent and precursor used (Figure 1C). Presumably, it is due to differences in viscosity and coordination nature of the solvents as well as the formation of intermetallic and Zintl phases with different molar volumes.[12] The prevalence of the nanopowder may be attributed to the destruction of microspheres, since the structural stability of the unprocessed materials is relatively low. Annealing can be used to improve the structural stability of the material as well as the crystallinity of target product;[14] however, it does not entirely prevent microsphere destruction.

The elemental composition of the unprocessed materials is represented by the targeted elements (C, Si, Ge, Sn, Sb) and O, Na, K and Cl. The phase composition of each crude product was determined using XRD, and the results showed that KCl was the dominant phase with NaCl impurities (Figure S2A, Tables S9 – S13). The higher proportion of K in the unprocessed product (Table S8) confirms the reaction mechanism because the reducing agent with lower redox potential, K, is entirely consumed before Na starts to react. The absence of target materials peaks combined with the EDX results indicates that the resulting metals/metalloids and their oxides are amorphous in the crude state. C-, Si-, Ge-, and Sb-based materials did not form crystalline phases of pure metalloids or their oxides and exist as amorphous “filler” uniformly distributed among crystalline KCl and NaCl (Figure S3). The Sn-based materials were the only samples that contained crystalline tin in the crude product. Since NaCl and

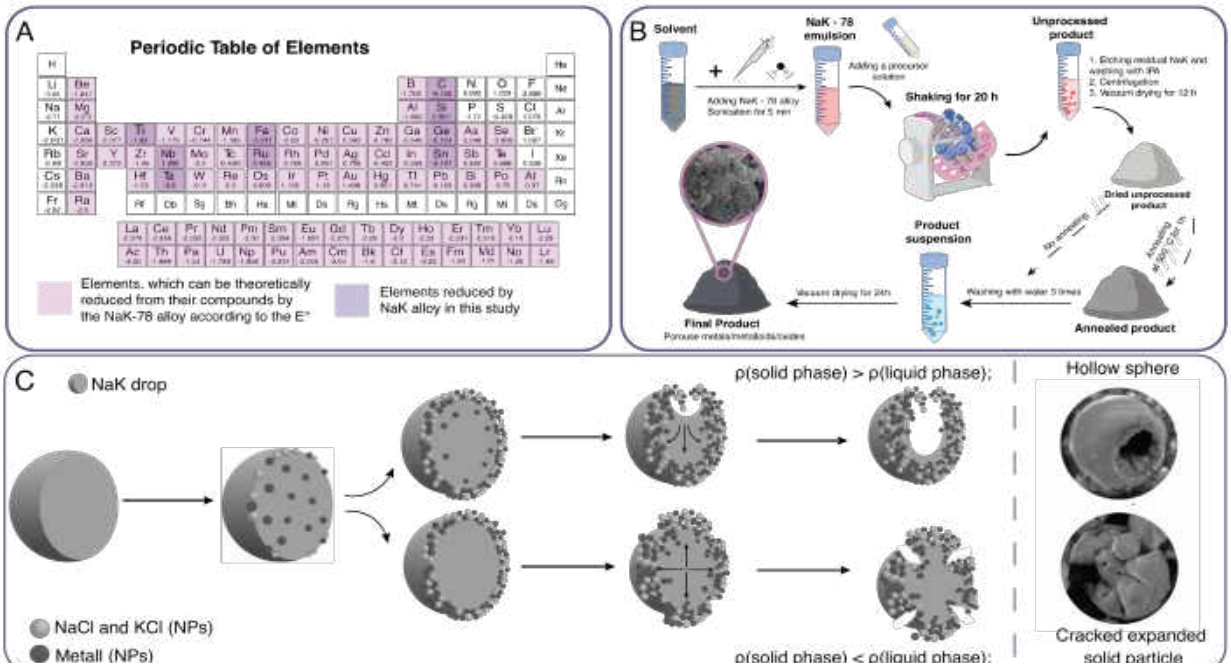

Figure 1. Scheme of the synthesis and research overview. (A) Periodic table with the highlighted elements, which can be theoretically obtained by the NaK-mediated chemical reduction in non-aqueous solutions. (B) General synthesis scheme of the proposed approach. (C) Supposed mechanism of the unprocessed product microspheres formation. E^0 is a standard electrode potential of an element (V); ρ is a density of phase (g·cm^{-3}).

KCl act as pore-forming agents, their crystallite sizes could be used as an approximate method for indirect pore size estimation in the proposed approach (Figure S2C).[21] The mean crystallite size for all the samples is 53.4 ± 2.6 nm (n = 40, p = 0.95), which might reflect macropore formation.

After annealing and removal of NaCl and KCl, the resulting nanostructures (final products) mainly degrade to nanoparticles. For C-, Si-, and Ge-based materials, the amorphous phases are reflected in the XRD pattern as halos or broad peaks (Figure S3). Presumably, these samples are represented by amorphous elementary substances, oxides, or their composites,[22] which is consistent with the EDX results. Conversely, the Sb- and Sn-based materials possess crystalline elementary substances on a par with crystalline oxides. The presence of the oxides is due to the washing of the oxygen-sensitive crude nano-architectures under ambient conditions, which leads to their oxidation. The yields of the unprocessed and final products differ significantly (Tables S9 – S13). While the crude products had a potential yield of 98% (Ge-based), the yield of the final products did not typically exceed 35% (Sn-based). Furthermore, the best results correspond to the samples obtained in DME media. Between hexane, xylene, and DME, the last one seems to be the best reaction media, providing the highest yield and reaction rate.

To evaluate the ability of the synthetic method to form porous materials, nitrogen sorption analysis was performed for the set of samples synthesised in DME media. The analysis confirmed the mesoporous structure of the materials, which was reflected in the hysteresis loop of the isotherms (Figure S4). The C-based material had the largest specific surface area, which was 2156 m^2/g (Table S15).

The remainder study concerned scaling and obtaining higher yields. To achieve that, we changed the reaction media. As it was shown, xylene gives us the most stable NaK emulsions and DME results in the highest yields. Therefore, we used another solvent, diglyme (DGM), since its chemical structure is similar to that of DME and its viscosity is close to that of xylene (Table S1).[23,24] In this case, we expanded the scope of the proposed synthetic approach to include Sn-, Sb-, Fe-, Ru-, Ta-, Nb-, and Ti-based materials. This was conducted without annealing (Table S13) and with the use of sonication to shorten the reaction time from 20 h to 2 h.[25] Ultrasonic allows to accelerate the precursors diffusion and the reaction, as well as to improve the contact area of reactants. $SnCl_4$, $SbCl_3$, $FeCl_3$, $RuCl_3$, $NbCl_5$, $TaCl_5$, $TiCl_4$ were used as precursors, and their respective solutions had concentrations of 0.10 M, which is higher than what was previously used. This way we doubled the mean yield (up to 70%). The resulting unprocessed and final samples were rough, shapeless, and mostly did not contain spherical particles. Thus, if there is no need to obtain microspheres, sonication helps to accelerate the reaction and improve reaction yield. Most of the samples contained macropores that were 80 – 150 nm in size, which were shown in the SEM micrographs (Figure 2, Figure S5). The porosities of the samples differ: the specific surface area for DME-synthesised Sn was 129 m^2/g while that of diglyme-synthesised Sn was 36 m^2/g (Table S15). Such a difference in specific surface area at almost similar pore size can be attributed to the higher viscosity of the diglyme, which decreases precursor diffusion and affects the mechanism of pore formation. These materials also have mesoporous structure (Figure S2B). The phase compositions of the obtained materials (Figure S3) are very similar to those of the prior ones, and depend on the availability of oxygen in the air. According to XRD, EDX, and additional FTIR spectroscopy (Figure S6), oxides were obtained for Ge, Sb, Ru, Fe, Nb, Ta, and Ti. However, Sn and Sb were again partially obtained in their metallic forms despite the exposure to air.

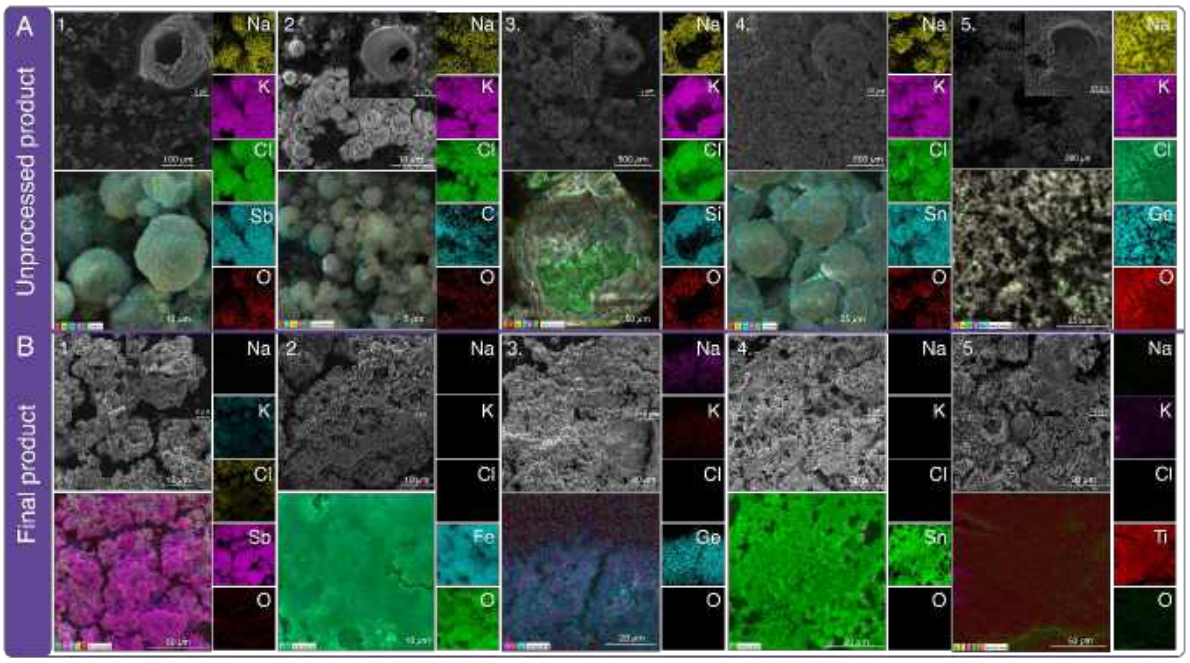

Figure 2. SEM and EDX characterisation. (A) Unprocessed products synthesised in DME (1 – Sb-based; 2 – C-based; 3 – Si-based; 4 – Sn-based; 5 – Ge-based). (B) Final products synthesised in diglyme media (1 – Sb-based; 2 – Fe-based; 3 – Ge-based; 4 – Sn-based; 5 – Ti-based). Element ratios are presented in Table S16 (ESI).

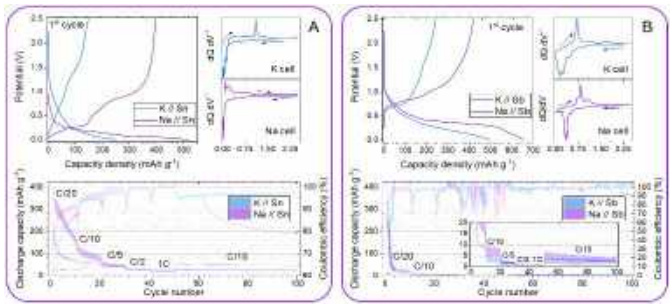

Figure 3. Anode materials testing. (A) Galvanostatic profiles of 1st cycles, their differential capacity plots, and cycling life (with deviations) of Na // Sn and K // Sn half-cells at C/20, C/10, C/5, C/2, 1C rates. (B) Galvanostatic profiles of 1st cycles, differential capacity plots, and cycling life (with deviations) of Na // Sb and K // Sb half-cells at C/20, C/10, C/5. C/2, 1C rates. The insert in the cycling stability curve is its zoomed in version.

In the final step of the research, we aimed to demonstrate the possibility of using the resulting products in energy storage device fabrication. Thus, the porous Sn- and Sb-based materials were incorporated as active components of Na- and K-ion batteries. Sn and Sb are widely known as alloying-type anode materials.[26] In Na-ion cells, Sn- and Sb-alloys form $Na_{15}Sn_4$ and Na_3Sb,[27] while in potassium-ion they form KSn and K_3Sb at full charge.[28] In this work, the porous structures were used to suppress anode expansion. Using our materials, we reached good cycling stabilities (91% after 50 cycles) and capacities of up to 353 mAh/g with a fading in the first 10 cycles at C/20 rate (see experimental details in the ESI).

In summary, we have presented an innovative and versatile platform for the template-free synthesis of metal- and metalloid-based porous materials. For the first time, NaK-78 emulsions were used as a sacrificial template to produce hollow nanostructured materials with adjustable porosity, morphology, and composition. We have shown that NaK acts as an agent for the chemical reduction, structure directing, and pore forming processes simultaneously. All the resulting nanomaterials possess macro- and mesoporous structures. The proposed approach is facile, scalable, and highly variable, making it suitable for many applications, including semiconductors, energy storage, and catalysis.

This work was supported by Russian Science Foundation Grant No. 24-23-00270. The authors thank the Priority 2030 Federal Academic Leadership Program for infrastructure support. P.A.M. gives thanks for the support by the RF Presidential scholarship. We also express gratitude to Leading Researcher (Institute for Problems in Mechanical Engineering RAS) Alexey Redkov for valuable consulting support.

Author Contributions

S.S.L. and N.V.G. performed the synthesis and characterization of the materials. S.S.L. and A.S.F. wrote the manuscript and illustrated it. P.A.M. fabricated the batteries and tested the synthesised materials as anodes. V.V.V. supervised the entire work and edited the manuscript.

Conflicts of interest

There are no conflicts to declare.

Notes and references

1 T. D. Bennett, F.-X. Coudert, S. L. James and A. I. Cooper, *Nat. Mater.*, 2021, **20**, 1179–1187.
2 I. G. Clayson, D. Hewitt, M. Hutereau, T. Pope and B. Slater, *Adv. Mater.*, 2020, **32**, 2002780.
3 X.-Y. Yang, L.-H. Chen, Y. Li, J. C. Rooke, C. Sanchezc and B.-L. Su, *Chem. Soc. Rev.*, 2017, **46**, 481–558.
4 T. Daeneke, K. Khoshmanesh, N. Mahmood, I. A. de Castro, D. Esrafilzadeh, S. J. Barrow, M. D. Dickeyb and K. Kalantar-zadeh, *Chem. Soc. Rev.*, 2018, **47**, 4073–4111.
5 J. Azadmanjiri, N. R. Thuniki, F. Guzzetta and Z. Sofer, *Adv. Funct. Mater.*, 2021, **31**, 2010320.
6 H. Wang, B. Yuan, S. Liang, R. Guo, W. Rao, X. Wang, H. Chang, Y. Ding, J. Liu and L. Wang, *Mater. Horiz.*, 2018, **5**, 222-229.
7 Y. Ding, Z. Deng, C. Cai, Z. Yang, Y. Yang, J. Lu, Y. Gao and J. Liu, *Int. J. Thermophys.*, 2017, **38**, 91.
8 A. S. Falchevskaya, A. Y. Prilepskii, S. A. Tsvetikova, E. I. Koshel and V. V. Vinogradov, *Chem. Mater.*, 2021, **33**, 1571–1580.
9 E. A. Sharova, A. S. Falchevskaya, S. S. Leonchuk, A. V. Redkov, V. Nikolaev and V. V. Vinogradov, *Chem. Commun.*, 2023, **59**, 10928–10931.
10 Y. Ji, Z. Li, Y. Liu, X. Wu and L. Ren, *Micromachines*, 2022, **13**, 1292.
11 M. Zhang, L. Liu, C. Zhang, H. Chang, P. Zhang and W. Rao, *Adv. Mater. Interfaces*, 2021, **8**, 2100432.
12 F. Dai, J. Zai, R. Yi, M. L. Gordin, H. Sohn, S. Chen and D. Wang, *Nat. Commun.*, 2014, **5**, 3605.
13 D. Tang, S. Hu, F. Dai, R. Yi, M. L. Gordin, S. Chen, J. Song and D. Wang, *ACS Appl. Mater. Interfaces*, 2016, **8**, 6779–6783.
14 D. Tang, T. Wang, W. Zhang, Z. Zhao, L. Zhang and Z.-A. Qiao, *Angew. Chem. Int. Ed.*, 2022, **61**, e202203967;
15 D. Tang, H. Yu, J. Zhao, W. Liu, W. Zhang, S. Miao, Z.-A. Qiao, J. Song and Z. Zhao, *J. Colloid Interface Sci.*, 2020, **561**, 494–500.
16 S. S. Leonchuk, A. S. Falchevskaya, V. Nikolaev, V. V. Vinogradov, *J. Mater. Chem. A*, 2022, **10**, 22955–22976.
17 CRC Handbook of Chemistry and Physics, ed. W. M. Haynes, CRC Press, 92nd edn, 2011.
18 G. Wilkinson, C. A. Murillo, M. Bochmann and F. A. Cotton, Advanced inorganic chemistry, John Wiley & Sons, 6th edn, 1999.
19 N. N. Greenwood and A. Earnshaw, Chemistry of the Elements, Elsevier, 2nd edn, 1997.
20 D. Tang, R. Yi, W. Zhang, Z. Qiao, Y. Liu, Q. Huo, D. Wang, *Mater. Lett.*, 2017, **198**, 140–143.
21 Y. Ishii, Y. Nishiwaki, A. Al-zubaidi and S. Kawasaki, *J. Phys. Chem. C*, 2013, **117**, 18120−18130.
22 F. Dai, R. Yi, M. L. Gordin, S. Chena and D. Wang, *RSC Adv.*, 2012, **2**, 12710–12713.
23 S. Tang and H. Zhao, *RSC Adv.*, 2014, **4**, 11251-11287.
24 R. A. Bley and S. M. Kauzlarich, *J. Am. Chem. Soc.*, 1996, **118**, 12461–12462.
25 Z. Li, J. Dong, H. Zhang, Y. Zhang, H. Wang, X. Cui and Z. Wang, *Nanoscale Adv.*, 2021, **3**, 41–72.
26 Y. Gu, Y. R. Pei, M. Zhao, C. C. Yang and Q. Jiang, *Chem. Rec.*, 2022, **22**, e202200098.
27 H. Xie, W. P. Kalisvaart, B. C. Olsen, E. J. Luber, D. Mitlinc and J. M. Buriak, *J. Mater. Chem. A*, 2017, **5**, 9661–9670.
28 J. Zhang, L. Lai, H. Wang, M. Chen and Z.X. Shen, *Mater. Today Energy*, 2021, **21**, 100747.